



Characterization and fracture toughness evaluation of the thick-walled wire arc additively manufactured low alloy steels

Kadir Dağyikan¹ · Uğur Gürol^{2,3} · Mustafa Koçak¹

Received: 19 August 2022 / Accepted: 18 November 2022
© International Institute of Welding 2022

Abstract

Wire arc additive manufacturing (WAAM) has recently gained great attention in producing metallic parts due to significant cost savings, high deposition, and its convenience. However, there is still limited knowledge concerning testing for mechanical properties of the WAAM-produced steel parts using different welding wires. This paper presents the results of the extensive experimental study aimed at assessing the mechanical properties of the WAAM-produced multi-pass thick-walled steel parts using two different ER70S-6 and one ER110S-G welding wires. This study focused on revealing the role of the microstructure on the fracture toughness values, which were obtained from the specimens extracted in two directions, namely, transversal direction (T) and longitudinal direction (L) according to the deposition direction. Before extraction of the toughness specimens, the computed radiography (CR) tests were performed to detect if any welding defects occurred during the layer deposition. Next, the microstructural features of the thick-walled WAAM parts were characterized by stereo microscopy (SM), optical microscopy (OM), and scanning electron microscopy (SEM). Finally, the mechanical properties of the part were evaluated by Charpy V-notch (CVN) impact toughness, tensile, and hardness tests. The results exhibit an anisotropic material behavior in as-built conditions for each filler metal. Therefore, careful consideration of notch orientations and their effects on mechanical properties is important in assessing the fitness-for-service performance of the WAAM-produced low-alloyed steel parts.

Keywords Direct energy deposition · Wire arc additive manufacturing · Welding wire · Low-alloyed steels · Fracture toughness

1 Introduction

Wire arc additive manufacturing (WAAM) using gas metal arc welding (GMAW) as a heat source has gained great attention in producing metallic parts due to significant cost

savings, high deposition rate, a larger selection of available wire materials, and convenience of WAAM processing [1, 2]. The use of welding wire instead of metal powder provides several advantages, such as a wide range of readily available wire materials with relatively lower prices than metal powders, as well as less health hazards during handling processing of the metal powders and simplified storage of wires compared to metal powders. Therefore, the WAAM process has been investigated in terms of technological performance, optimization of process parameters, and metallurgical properties of the metallic parts, including low C-Mn steels [3], duplex stainless steel [4], AISI H13 tool steel [5], Inconel 625 [6], Al 4043 alloy [7], Ti-6Al-4 V alloy [8], and copper alloys [9] under the direct energy deposition (DED) method of the additive manufacturing technology.

Although WAAM is accepted to have some significant advantages, one of the drawbacks of this technique is high heat input, which results in the serious thermal accumulation with the successively deposited layers. Therefore, the

Recommended for publication by Commission I - Additive Manufacturing, Surfacing, and Thermal Cutting

This study was presented at the 75th IIW Annual Assembly and International Conference on 16-22 July 2022

✉ Uğur Gürol
ugur.gurol@yahoo.com

¹ Department of Mechanical Engineering, İstanbul Gedik University, İstanbul, Turkey

² Department of Metallurgical and Materials Engineering, İstanbul Gedik University, İstanbul, Turkey

³ Gedik Welding Inc., Research and Development Center, İstanbul, Turkey

microstructure and mechanical properties can significantly be influenced in each direction, which is an anisotropy. In fact, the anisotropy phenomenon in the microstructure is not only a problem in WAAMed parts but also an issue in all additively manufactured parts; hence, it has attracted attention of many researchers to work on it. Sun et al. [10] investigated the anisotropic behaviors of a thin-walled WAAM-produced steel part via mechanical testing performed in the building (vertical) and welding (horizontal) directions. They found that the yield strength, tensile strength, and elongation values of the specimens taken horizontally are greater, about 10.1%, 4.2%, and 21.4%, than those of specimens taken vertically. However, Le and Paris [11] reported that the yield and tensile strength of the ER70S-6 wall produced with 60 s idle time between the layers in the horizontal direction were lower by about 11.6% and 10.4% than that of specimens extracted in the vertical direction. Le et al. [12] demonstrated that lower yield and tensile strengths were found in horizontal specimens, while ductility was higher than in vertical ones. Yildiz et al. [2] have studied the effect of WAAM process parameters by changing the wire feed speed, travel speed, and their ratio on the single-bead welds of HSLA steel and kept the idle time to 60 s. as a constant. They reported that the yield and tensile strength values obtained from the specimens taken horizontally and vertically of the WAAM wall were similar. In contrast, elongation values of the WAAMed parts exhibited slight differences, lower than 10%. Aldalur et al. [13] compared the microstructural and mechanical properties of thick-walled mild steel (ER70S-6 wall) produced with oscillatory and overlapping weld pass strategies. They reported similar tensile and impact properties; however, both strategies had higher elongation values of up to 10% in horizontal directions. In addition, Plangger et al. [14] indicated there are no significant signs of anisotropy regarding tensile strength, impact, and fracture toughness for the fine-grained steels with a yield strength of 890 MPa obtained by the CMT WAAM process using a micro-alloyed solid wire. Furthermore, Silwal et al. [15] investigated the effect of the varying concentrations of Ar and CO₂ shielding gas blends to modify the local micro-mechanical properties of the WAAM-produced C-Mn steels. They reported that the strength and ductility of ER70S-6 wire were within 460–480 MPa and 30–38%, respectively. However, no significant differences in the tensile properties between the test samples extracted in longitudinal and transverse directions, except for the use of shielding gas with 2% CO₂. Refieezad et al. [16] studied the GMAW-based WAAM process to produce thin-walled low-alloyed steel structures using ER70S-6 welding wire. They indicated that the ductility in the horizontal direction was found to be approximately three times higher than that of the vertical direction due to the occurrence of a coarse grain structure in the HAZ and the formation of local brittle zones (LBZs

known as Martensite-Austenite constituent) at the inter-pass regions and the melt-pool (as-welded microstructural region) boundaries in the vertical direction.

As seen in the previous studies, most studies have been carried out on the thin-walled (use of single wire) WAAM materials. The results of the microstructural and mechanical characterization have revealed strong anisotropic behaviors (directional dependence on the build-up and welding directions) on tensile properties and reported differences in vertical and horizontal directions of the thin WAAM-Wall. These reported test results as “directionality” in mechanical properties of the WAAM steel materials should be studied in detail, especially in thicker parts, to be more interesting for the structural applications. There is still limited knowledge concerning the Charpy-V impact toughness of the thin and/or thick-walled WAAM-produced steel parts. This paper, therefore, presents the results of the extensive experimental study aimed at assessing all mechanical properties (including standard Charpy-V fracture toughness properties) of the WAAM-produced multi-pass (three passes next to each other) thick-walled steel parts using two different ER70S-6 and one ER110S-G class welding wires. The specific aim of the study was to establish a relationship between microstructure and Charpy-V fracture toughness properties of the thicker WAAM-Wall materials. The study focused on revealing the role of the microstructure on the fracture toughness values obtained from the specimens extracted in two directions, namely, transverse (T) and longitudinal directions (L).

2 Materials and method

The 12-mm thick S355J2-N grade steel plates were used as a substrate to produce robotic wire arc additive manufactured (WAAM) parts. Two different ER70S-6 class and one higher strength ER110S-G class welding wires according to AWS A5.18 and AWS A5.28 with 1.2-mm diameter were used as the filler materials. While the SG2-wire, classified as one of the ER70S-6 wires, is used for joining the mild and medium tensile steels to obtain comfortably high impact toughness values down to -20 °C temperature, the SG3-wire is used for structural applications needing higher tensile strength. The increased strength of the SG3 wire is achieved by increasing the silicon and manganese contents of the wire compared to the SG2 wire. The third wire used in this study, ER110, is also used for higher-strength structural steel applications. The higher strength is simply due to the use of higher amounts of Mn, Mo, Ni, and Cr elements in the wire. Selecting these three different welding wires aimed to obtain distinctly different microstructures, hardness, tensile properties, and Charpy-V fracture toughness values to study isotropic behaviors of the thicker structural steel WAAM parts.

The chemical compositions (wt.%) of the filler metals obtained by optical emission spectroscopy were given in Table 1.

The WAAM process was carried out with a robotic gas metal arc welding (GMAW) process using a low spatter process with the following parameters: an arc current of 185 A, an arc voltage of 18 V, a wire-feeding speed of 4.7 m/min, a travel speed of 8.5 mm/s, and Ar + 18% CO₂ mixed gas as the shielding gas with the flow rate of 15 L/min. GeKa-Mac WB 500 L GMAW welding machine with a water-cooled torch mounted on a 6-axis OTC Daihen FD-V8L industrial robot was used as the power source of the process, and the base plate was clamped to the working table before the welding process to minimize the potential distortion due to the thermal input as shown in Fig. 1.

The deposition strategy during the fabrication of thick-walled samples is shown in Fig. 2. Three single passes were continuously deposited with stringer mode next to each other and formed a layer. The following passes were deposited with a 30–35% overlap ratio next to the previous pass and pass directions were reversed each time to avoid build-up at the start and end of the paths. Then, the torch was ascended to a height of 1.7 mm after each layer to obtain the thick-walled layers. The deposition process was repeated on top of the previous layer until the total height of the WAAM part reached about 60 mm. The thickness of the WAAM part was aimed to reach about 15–16 mm to obtain standard size (10 × 10 × 55 mm) Charpy-V fracture toughness test specimens in all directions to study the isotropic behavior of the WAAM-manufactured low-alloyed steels.

Gürol et al. [3] reported that the continuous deposition results in heat build-up and this slows down the cooling rate, especially in the later layers. Their findings also given in the AWS A5.18 welding standard restricts inter-pass temperature at 165 °C during the conventional welding practices. Therefore, in our study, the deposition of the subsequent layer started after the temperature of the previous one cooled down to 135–165 °C, measured by an infrared (IR) thermometer in the middle of the last deposited layer. This Fluke 62 Mini IR thermometer is a non-contact diagnostic tool with a distance-to-spot ratio of 10:1 and capable of measuring from -30 °C to 500 °C accurately to ± 1% of reading. Furthermore, the surfaces of each layer were carefully cleaned by using a steel wire



Fig. 1 The robotic cell for wire arc additive manufacturing (WAAM) process with GMAW welding machine

brush to avoid any remaining slag from the previous weld- ing pass before later depositions.

Upon the completion of the manufacturing of WAAM- produced wall parts, computed radiography tests were per- formed according to EN ISO 17636–2 to detect if any inter- layer welding defects were present which may occur during the layer depositions. The mechanical properties of the parts were evaluated with hardness, flat tensile, and Charpy V-notch (CVN) impact toughness test results. The hardness tests were performed according to EN ISO 9015 using a fully automatic hardness device with the Vickers (HV) method under a load of 5 kgf. The uniaxial tensile tests were conducted at room temperature using sub-size flat type tensile specimens accord- ing to ASTM E8. The locations and positions of the speci- mens extracted are shown in Fig. 3. The CVN samples were extracted from two directions shown: horizontal (parallel to the deposition direction) and vertical (perpendicular to the

Table 1 Chemical analysis of the welding wires used (wt.%)

Wire	Classification	C	Si	Mn	Mo	Ni	Cr	Cu
SG2	ER70S-6	0.07	0.85	1.46	0.001	0.015	0.022	0.02
SG3	ER70S-6	0.08	0.92	1.72	0.001	0.039	0.020	0.05
ER110	ER110S-G	0.10	0.54	1.75	0.254	1.455	0.265	0.05

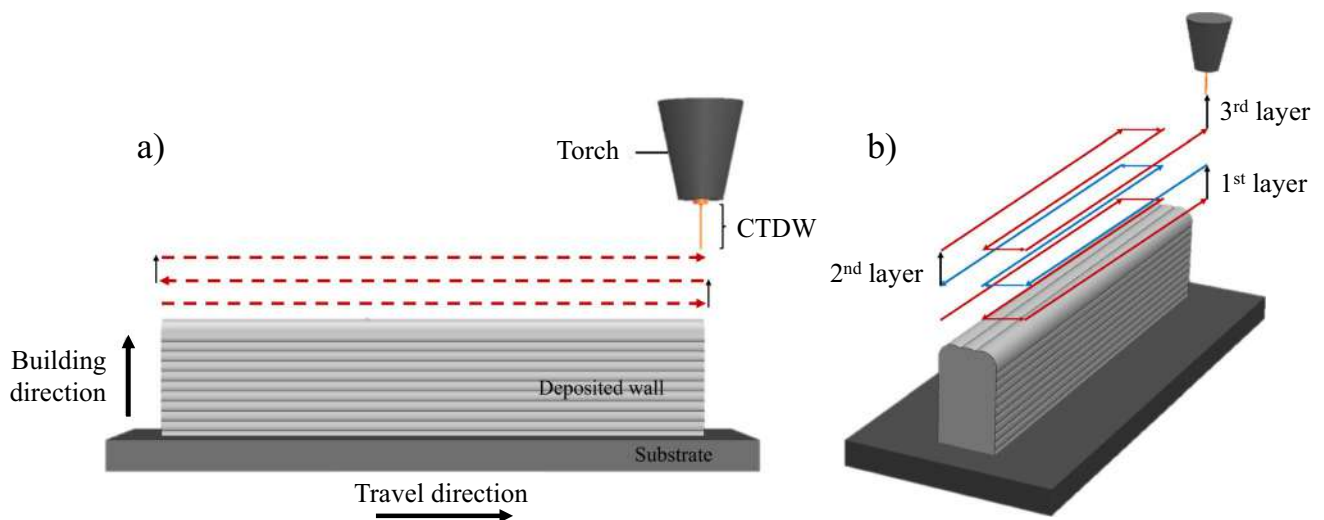


Fig. 2 Deposition strategy for thick-walled (16 mm) WAAMed parts made of three side-by-side passes and 27 layers in building direction to reach 60 mm height; (a) front view and (b) side view

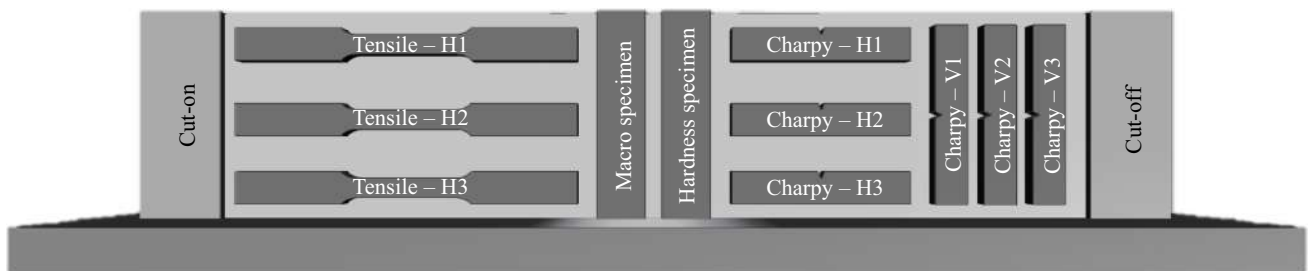


Fig. 3 The locations of the test specimens on the 16 mm thick WAAM-Wall steel material. The length of the wall was 320 mm while height of the wall was approx. 60 mm with the thickness of 16 mm

deposition direction). The CVN tests were performed at a test temperature of $-20\text{ }^{\circ}\text{C}$ according to EN ISO 9016. Standard metallographic procedures (such as grinding, polishing, and etching) for the cross-sectional specimens were performed according to ISO 17639 to reveal the microstructural features and changes depending on filler metals and location of the layers. The macro and micro-structural features of the thick-walled WAAM parts are characterized by using stereo microscopy (SM), optical microscopy (OM), and scanning electron microscopy to reveal characteristics of all three WAAM parts manufactured using different welding wires.

3 Results and discussion

Figure 4a-c shows computed radiography test results of the thick-walled WAAM-produced parts. No weld between the layers and side-by-side passes was detected in all three parts. Three welding passes side by side were used to build up the WAAM part to obtain a 16-mm thick parts. The length,



Fig. 4 Computed radiography test results of WAAM-produced parts using (a) SG2, (b) SG3, and (c) ER110 welding wires

height, and thickness of the WAAM parts obtained with 27 layers were measured as 320, 60, and 16 mm, respectively.

Figure 5 shows the macro-section views of the WAAM-produced three parts. No significant defect in the forms of pores, cracks, or improper fusions between the adjacent layers was found. These findings confirm that the robotic GMAW-based WAAM process has the capacity to build thicker wall steel parts with good bonding / interlayer strength between the layers, without any welding defects, provided the use of optimum process parameters and welding wires.

The optical micrographs of WAAM-produced parts taken from the middle section of the wall were displayed in Fig. 6. The micro-structures of WAAM walls produced with SG2 and SG3 wire were found to be consisting polygonal ferrite (PF) with a small amount of pearlite at the grain boundaries due to continuous recrystallization by successive layers (Fig. 6a-d). The average grain size of PF grains in the middle region of SG2 wire was measured as 13.61 ± 1.27 , whereas that of SG3 wire was 11.31 ± 1.30 , using the intercept method according to ASTM E112. Similar microstructures were also reported in a previous study [12, 16]. This microstructure is also typical of plain carbon steel with a low carbon content such as St37 and St52 [17]. On the other hand, the microstructure of side regions for WAAM

parts consists of a columnar and reheated region (Fig. 5a-b). The varying ferrite structures such as acicular ferrite (AF), grain boundary ferrite (GBF), and ferrite side plates (FSP) occurred inside regions in addition to polygonal ferrite for SG2 and SG3 wires. However, the amount of AF increased, and the thickness of the GBF decreased in SG3 compared to SG2 wire, which is beneficial development in terms of fracture toughness of the SG3 microstructure. Moreover, the part produced with the high strength ER110 welding wire consists mainly of an acicular ferrite structure with a small amount of the bainite and martensite–austenite (M–A) constituents, as shown in Fig. 6e-h. The formation of bainite occurred due to the fast-cooling rate involved during solidification [18].

Figure 7 shows the hardness distribution of the parts produced with three welding wires. The hardness points were set in a line in the middle of the part along the building direction with an interval of 0.5 mm. The average hardness for SG2, SG3, and ER110-produced parts were found to be 155 ± 4 , 163 ± 5 , and 286 ± 10 , respectively, confirming a homogenous hardness distribution along the building direction due to similar inter-layer temperatures occurred during the build-up processes of 27 layers. The part produced with SG3 wire showed a slightly decreasing trend of hardness with the distance from the substrate (up to 15 mm), while

Fig. 5 The macro-structure of the WAAM-produced parts using (a) SG2, (b) SG3, and (c) ER110 welding wires

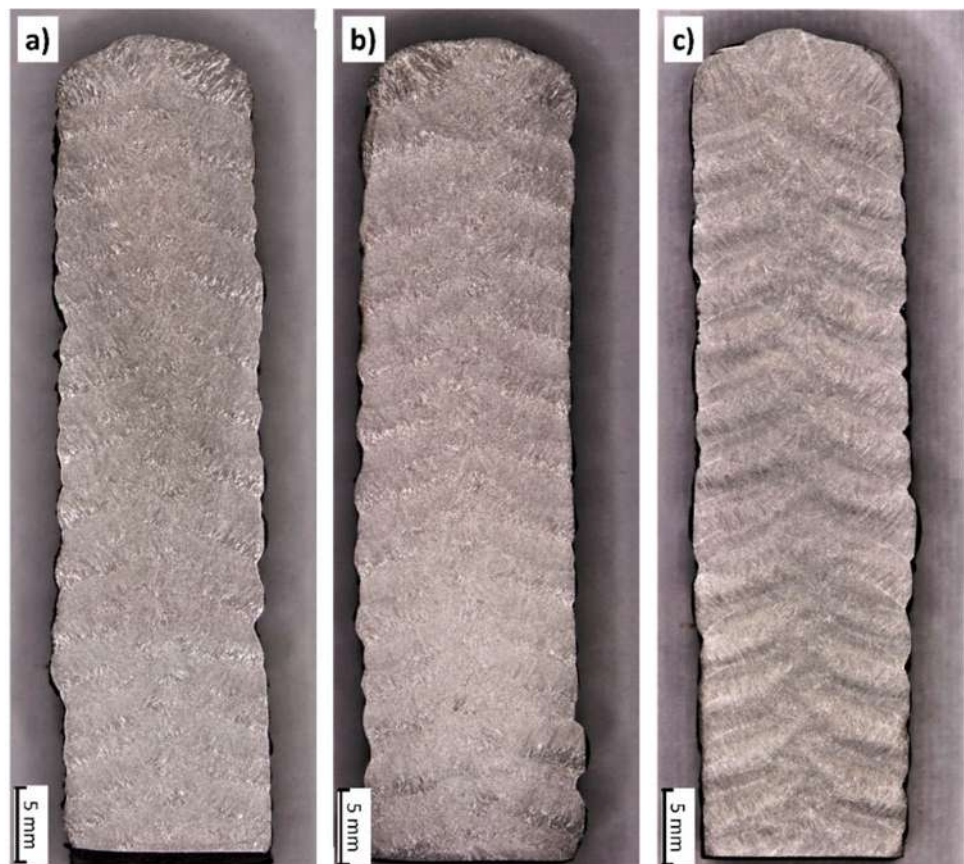
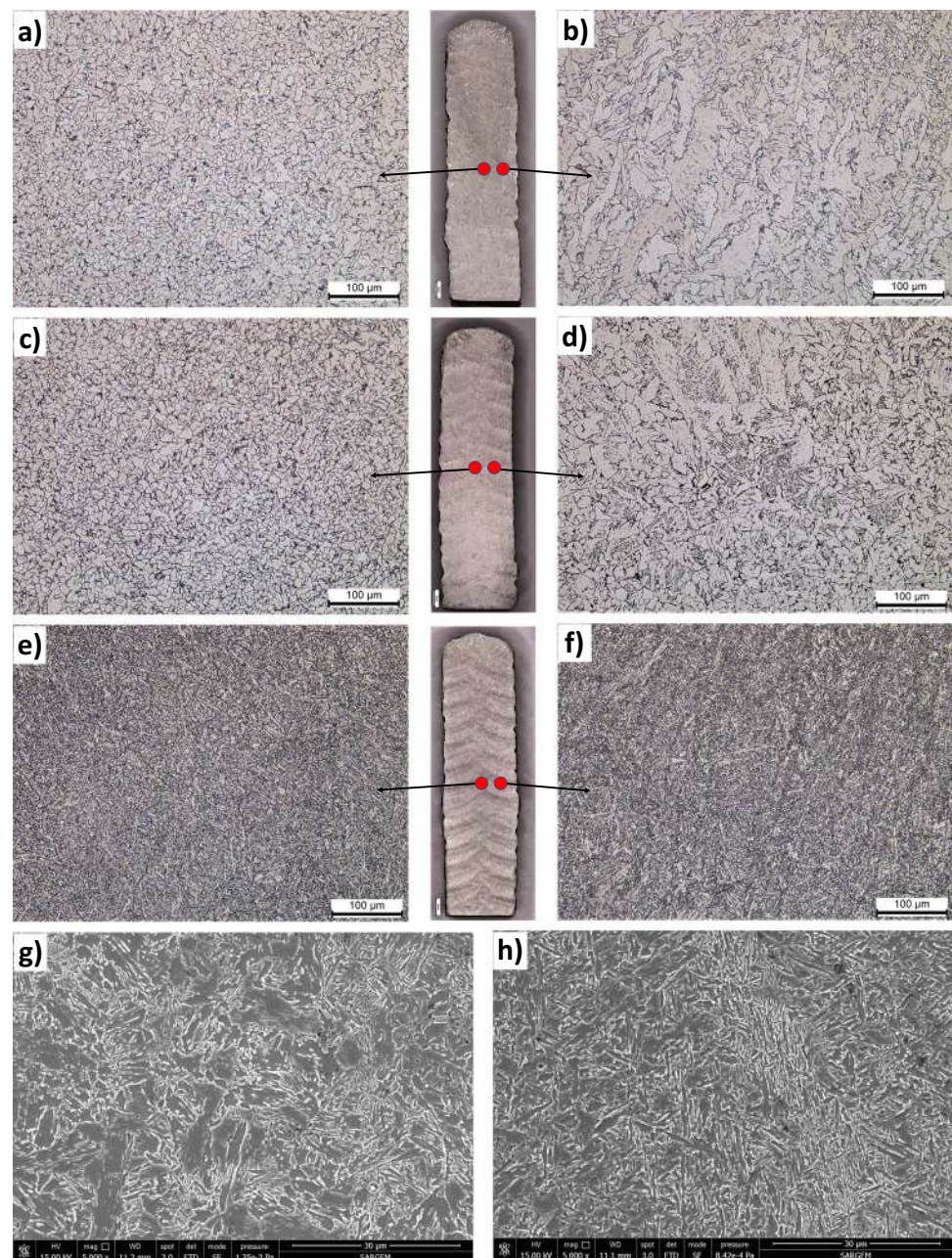


Fig. 6 The optical micrographs of WAAM-produced parts; (a, b) SG2, (c, d) SG3, (d, e) ER110, and (g, h) detailed SEM microstructures of the ER 110 welding wire



parts produced with SG2 and ER110 showed a relatively constant trend. This variation can be attributed to the slight change in the inter-layer temperature that tried to keep within the range of 135 – 165 °C and the ambient temperature that directly influence the cooling rate of the parts. Moreover, the hardness values obtained from the center lines of the WAAM parts are showing less variation for all three welding wires (solid symbols), compared to side regions (Fig. 7a-c). This is due to the responses of the differences in the microstructures to the relatively higher cooling cycles at the near-edge regions. Whereas open triangle symbols showed the microstructural nature of the multi-pass layers,

which have as-welded columnar weld metals and refined micro-structural regions with subsequent layers which in turn exhibit different hardness values. The thermal cyclic heating, which causes the hardening and softening of adjacent layers, is responsible for the hardness variations in all WAAM-walls. Similar hardness trends were reported in the WAAM structure built with structural steel parts [19–23]. However, the hardness values obtained for the WAAM part produced with ER110 wire are lower than the expected martensitic hardness of around 350 HV for carbon steel with around 0.1 wt.% C [24], which is good in agreement with Fig. 6e-h.

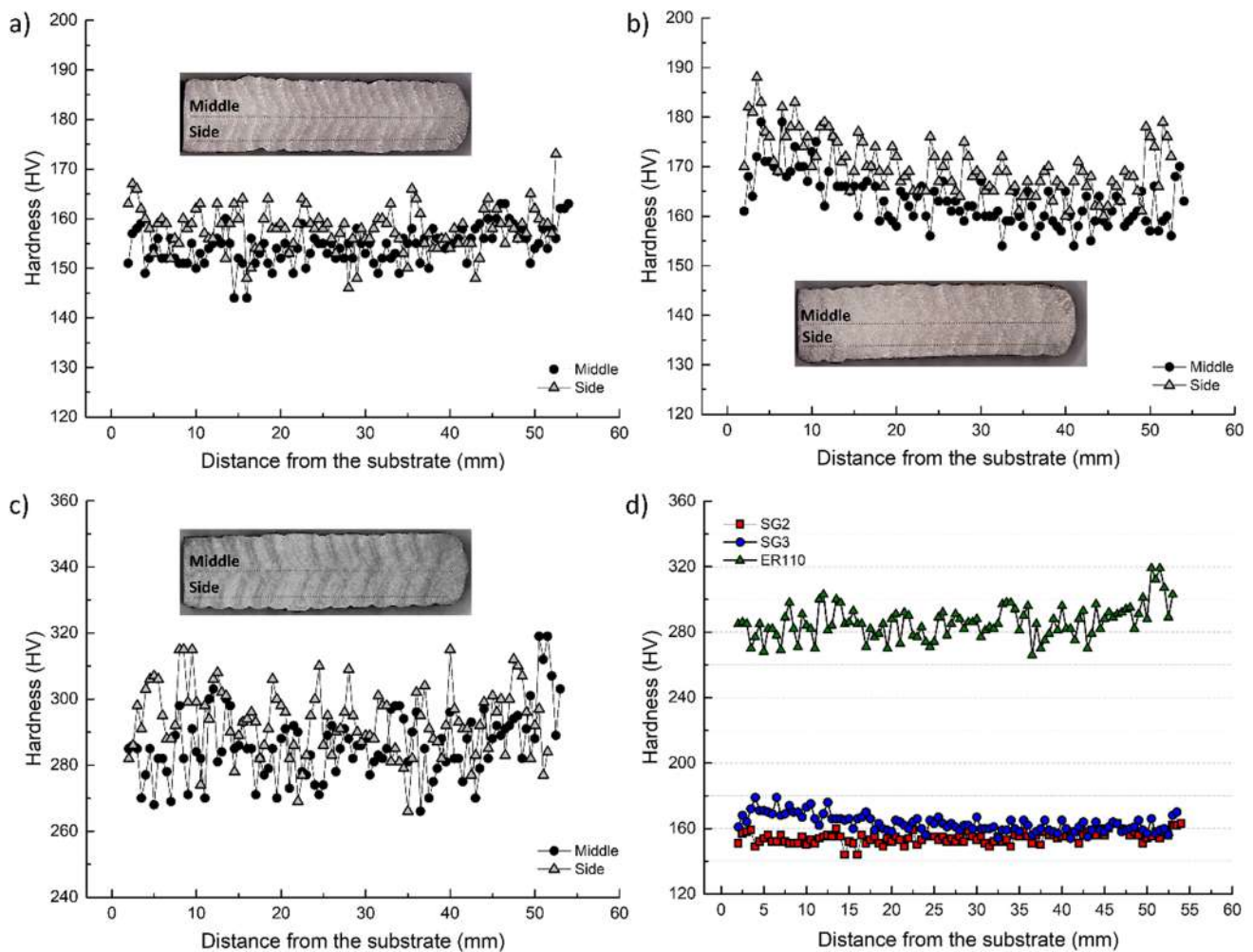


Fig. 7 Hardness distributions of 16 mm thick WAAM-parts with varying welding wires throughout building direction. **a**, **b**, and **c** are showing the hardness values of SG2, SG3, and ER110 welding wires

at mid-section and side of the parts, respectively. **d** shows the comparison of the hardness values of three welding wires. Note that the higher strength welding wire ER 110 reveals higher hardness values

The tensile test results obtained at an ambient temperature depending on the specimen locations were listed in Table 2, and the results were compared in Fig. 8. The strength and elongation values of the welding wires obtained from the standard welding process (manufacturer values) are also shown in Table 2 for all three wires. This comparison is essential concerning designing the WAAM parts for manufacturing structural load-bearing parts using these wires. Sufficiently high and consistent (all three locations) tensile properties were obtained from 16 mm thick, three passes each layer WAAM-Wall materials as shown in Table 2. It is obvious that the WAAM type of manufacturing of the structural parts can yield comparable tensile properties to the standard weld metal produced originally for the joining of the parts. These results clearly show that conventional SG2 and SG3 welding wires as well as higher strength welding wire of ER110 can be used to manufacture thick structural steel WAAM parts.

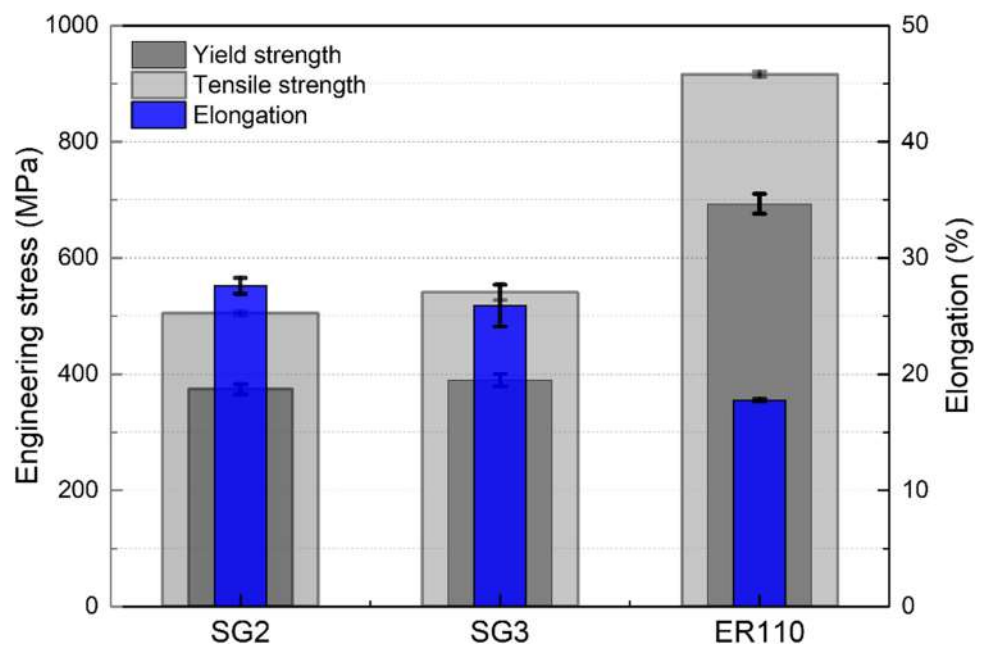
The CVN test results obtained at $-20\text{ }^{\circ}\text{C}$ test temperature using two notch directions as shown in Fig. 3 and varying specimen locations (in 60 mm wall height, Fig. 3) were listed in Table 3. It is essential to determine the toughness properties of the different locations of the WAAM-Wall since the thermal history of the part with increasing layers may differ if process parameters are not well-controlled in terms of inter-layer timing. Therefore, care was given to keep the time between the passes as constant as possible. By doing so, the microstructural and hence maximum homogeneity in mechanical property in all locations of the WAAM-Wall was achieved, as shown in Table 3 and Fig. 8. The comparison of CVN test results depending on the notch direction also was shown in Fig. 9. It was found that the impact toughness values of the CVN specimens extracted in the vertical direction were about 19%, 24%, and 21% higher than in horizontal direction for SG2, SG3, and ER110 wire, respectively. These results are somehow inevitable due to the layered structure

Table 2 Tensile test results depending on the location of the test specimens

Wire	Position	Yield strength (MPa)	Tensile strength (MPa)	Elongation (%)
SG2	Manufacturer	Min. 420	500- 640	Min. 22
	Top	367	506	27,08
	Middle	372	507	28,37
	Bottom	384	500	27,28
	Average	374±9	504±4	27.6±0.7
SG3	Manufacturer	Min. 460	540- 680	Min. 22
	Top	385	528	25,97
	Middle	382	538	27,64
	Bottom	402	554	24,02
	Average	390±11	540±13	25.9±1.8
ER110	Manufacturer	Min. 690	Min. 760	Min. 19
	Top	689	911	17,76
	Middle	679	920	17,87
	Bottom	712	918	17,66
	Average	693±17	916±5	17.8±0.1

of the WAAM process and its resulting microstructures. The designer should consider this fact and accordingly make the usage plan for the part to be manufactured by the WAAM process. All fracture toughness results at -20 °C have shown very good toughness levels, indicating that these WAAM parts can be used safely in structural (load-bearing) applications where high toughness values are needed for tolerances against the presence of crack-like defects and notches.

In order to verify the obtained Charpy-V test results, fracture surfaces were examined to identify the main types of fractures, whether the fracture types are ductile or brittle. Figure 10 shows the fracture surfaces of the Charpy-V specimens extracted from vertical (Fig. 10a, c, e) and horizontal (Fig. 10b, d, f) direction for SG2, SG3, and ER110 welding wires, respectively. As expected, all the specimens exhibited a mixture of shear and flat fracture regions. The detailed SEM micrographs taken from vertical (Fig. 7c) and horizontal (Fig. 7d) direction for the SG3 welding wire indicated that the shear regions were composed of fully ductile fracture while the flat regions were as ductile, brittle, or a combination of both. In this context, it can be clearly seen that the increased number of flat regions (shown with yellow lines) resulted in a decrease in toughness values. In other words, a higher amount of flat regions were identified in

Fig. 8 Tensile test results of the WAAM parts manufactured using 1.2 mm diameter three different welding wires**Table 3** CVN test results depending on the notch directions and location of the specimens manufactured using three welding wires

	SG2		SG3		ER110	
	Vertical (J)	Horizontal (J)	Vertical (J)	Horizontal (J)	Vertical (J)	Horizontal (J)
Top	150	117	159	138	78	85
Middle	144	117	179	136	88	75
Bottom	141	131	170	139	98	62
Average	145±5	122±8	170±10	137±2	88±10	73±10

Fig. 9 CVN test results of all three wires at -20 °C depending on the notch directions. See Fig. 3 for the notch directions

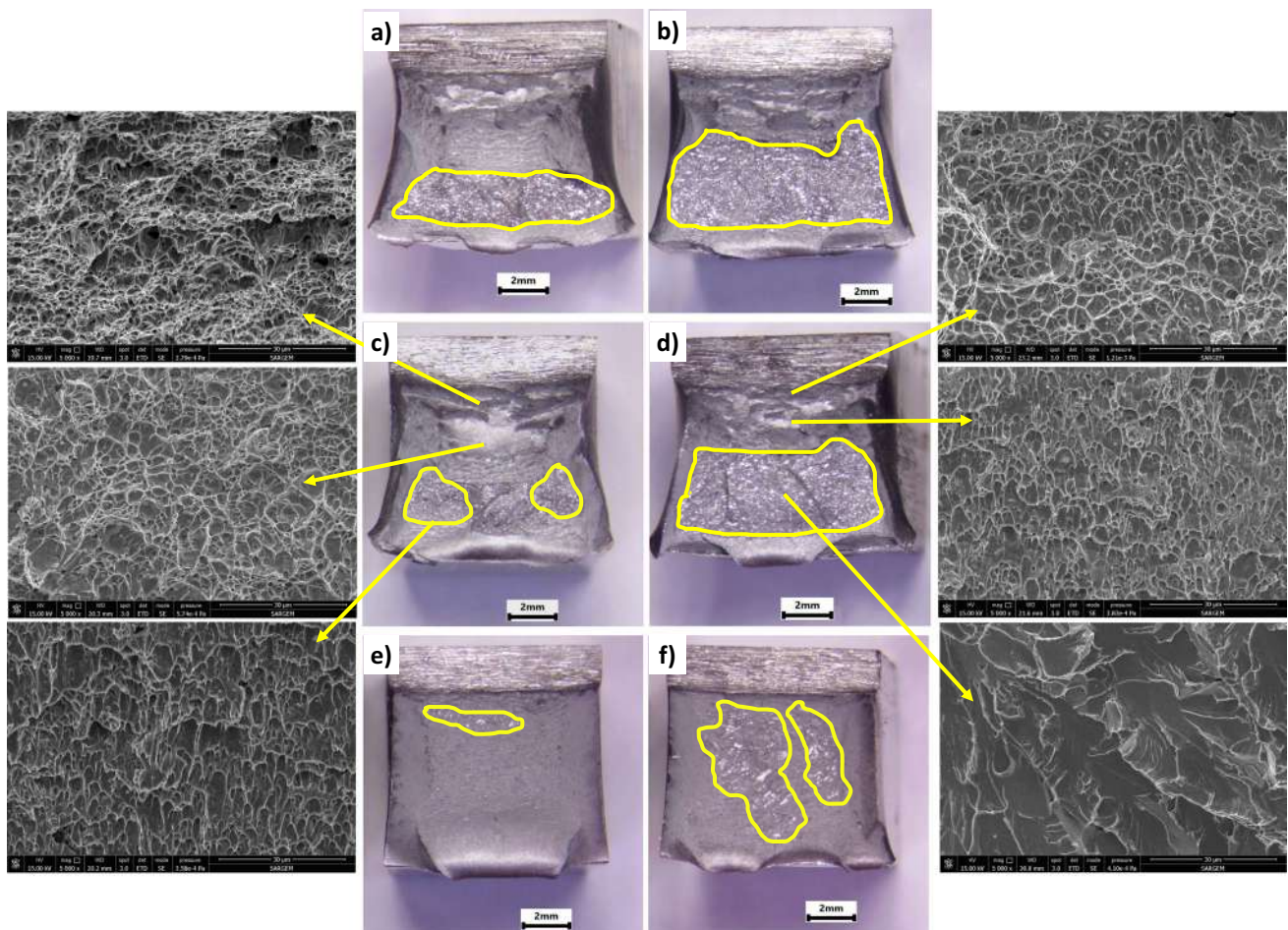
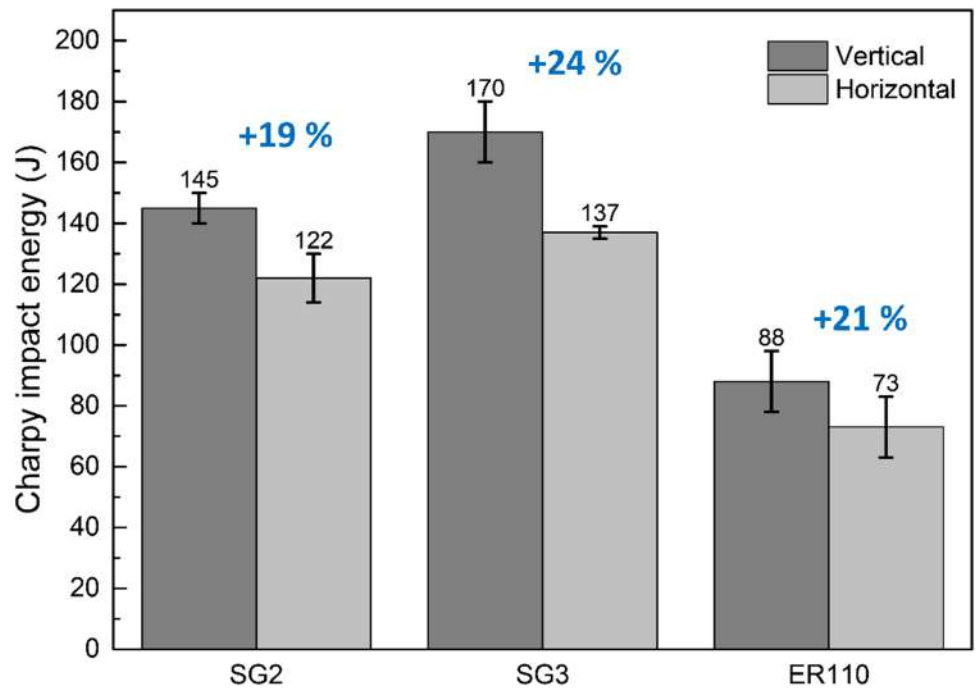


Fig. 10 Fracture surfaces of the Charpy-V specimens extracted from vertical (a, c, e) and horizontal (b, d, f) direction for SG2, SG3, and ER110 welding wires, respectively, which showing larger flat areas in horizontal specimens which has produced lower toughness values

Table 4 Comparison of the mechanical properties of the WAAM parts obtained within the scope of this study and standard steel grades [25, 26]

Grades	Yield strength (MPa)	Tensile strength (MPa)	Elongation (%)	Charpy impact energy (J, at -20 °C)
SG2-Wall	374 ± 9	504 ± 4	27.6 ± 0.7	122 ± 8
SG3-Wall	390 ± 11	540 ± 13	25.9 ± 1.8	137 ± 2
ER110-Wall	693 ± 17	916 ± 5	17.8 ± 0.1	73 ± 10
S235-J2	Min. 235	360–510	Min. 26	Min. 27
S275-J2	Min. 275	410–560	Min. 23	Min. 27
S355-J2	Min. 355	470–630	Min. 22	Min. 27
S690QL	Min. 690	770–940	Min. 17	Min. 40

horizontal specimens where lower toughness results were obtained, and this confirms the differences in toughness values where directional dependency exists.

Finally, mechanical properties of the WAAM parts are compared with some respective steel grades given in Table 4. SG2 and SG3 welding wires are usually used to weld low to medium strength level steel grades, such as 355 steel. ER110 welding wire corresponds to the higher strength steel, such as 690 MPa steel. As it can be seen in Table 4, WAAM parts exhibit comparable properties to the standard steel grades. These results and reported fracture toughness values are clearly showing the suitability of the WAAM process to manufacture load-bearing steel parts using %100 welding wires.

This on-going research project will be extending the work into the characterization and simulation of the residual stresses of these WAAM parts to determine the distribution and levels of the residual stresses. Furthermore, fracture toughness values will be examined in terms of crack tip opening displacement (CTOD) fracture toughness tests to generate toughness data that can be directly used in defect assessment and fitness-for-service (FFS) procedures.

4 Conclusions

The 16-mm thick WAAM parts were manufactured using 1.2-mm diameter three different welding wires, one of which was higher strength ER 110 welding wire. The main purpose of this study was to investigate the fracture toughness characteristics of these WAAM-Walls to demonstrate their suitabilities for structural applications.

The following conclusions can briefly be made.

- It is demonstrated that for all three welding wires, SG2, SG3, and ER110, WAAM process can be used to manufacture thick-walled (here is 16 mm) steel parts with good bonding strength between the layers, and without welding defects were obtained by GMAW-based WAAM process
- No visible deformation or deflection of the parts and occurrence of defects or imperfections was identified for all three wires due to the well-controlled WAAM process parameters
- The homogenous hardness distribution was found along the building direction for all parts. This can be attained by controlling the heat input and development of the temperature variation during the manufacturing of each layer
- The impact toughness values of the CVN specimens tested at the -20 °C test temperature extracted in vertical direction were found to be about 19%, 24%, and 21% higher than those of specimens positioned in horizontal direction for SG2, SG3, and ER110 wire, respectively. However, all three parts manufactured with commercially available welding wires have demonstrated good fracture toughness values (higher than 47 J enabling the classification of the welding wires according to EN standards utilizing a system based on the yield strength) sufficient for the structural applications in general engineering terms
- The obtained mechanical properties are clearly showing the suitability of WAAM process to manufacture load bearing thick steel parts and parts such as S235, S275, S355 and S690QL steels with the use of SG2, SG3, and ER110 welding wires

Acknowledgements The authors wish to acknowledge the valuable contributions of Mrs. Nurten Güleçyüz for conducting robotic welding operations. Sincere thanks will be extended to the Gedik Welding Company for the provisions of the robotic welding facilities and its members of the robotic laboratory and testing hall staff members for their support during the experiments.

Funding This research did not receive any specific grant from funding agencies in the public, commercial, or not-for-profit sectors.

Declarations

Conflict of interest The authors declare no competing interests.

References

1. Çam G (2022) Prospects of producing aluminum parts by wire arc additive manufacturing (WAAM). *Mater Today* 62:77–85. <https://doi.org/10.1016/j.matpr.2022.02.137>
2. Yildiz AS, Davut K, Koç B, Yılmaz O (2020) Wire arc additive manufacturing of high-strength low alloy steels: study of process parameters and their influence on the bead geometry and mechanical characteristics. *Int J Adv Manuf Technol* 108:3391–3404. <https://doi.org/10.1007/s00170-020-05482-9>
3. Gürol U, Dilibal S, Turgut B, Koçak M (2022) Characterization of a low-alloyed steel component produced with wire arc additive manufacturing process using metal-cored wire. *Mater Test* 64(6):755–767. <https://doi.org/10.1515/mt-2021-2155>
4. Wittig B, Zinke M, Jüttner S (2021) Influence of arc energy and filler metal composition on the microstructure in wire arc additive manufacturing of duplex stainless steels. *Weld World* 65:47–56. <https://doi.org/10.1007/s40194-020-00995-z>
5. Hackenhaar W, Mazzaferro JAE, Mazzaferro CCP (2022) N Grossi, G Campatelli (2022) Effects of different WAAM current deposition modes on the mechanical properties of AISI H13 tool steel. *Weld World*. <https://doi.org/10.1007/s40194-022-01342-0>
6. Mookara RK, Seman S, Jayaganthan R, Amirthalingam M (2021) Influence of droplet transfer behaviour on the microstructure, mechanical properties and corrosion resistance of wire arc additively manufactured Inconel (IN) 625 components. *Weld World* 65:573–588
7. Pramod R, Kumar SM, Girinath B, Kannan AR, Kumar NP, Shanmugam NS (2020) Fabrication, characterisation, and finite element analysis of cold metal transfer-based wire and arc additive-manufactured aluminium alloy 4043 cylinder. *Weld World* 64:1905–1919. <https://doi.org/10.1007/s40194-020-00970-8>
8. Xian G, Oh JM, Lee J, Cho SM, Yeom JT, Choi Y, Kang N (2022) Effect of heat input on microstructure and mechanical property of wire-arc additive manufactured Ti-6Al-4 V alloy. *Weld World* 66:847–861. <https://doi.org/10.1007/s40194-021-01248-3>
9. Baby J, Amirthalingam M (2020) Microstructural development during wire arc additive manufacturing of copper-based components. *Weld World* 64:395–405. <https://doi.org/10.1007/s40194-019-00840-y>
10. Sun L, Jiang F, Huang R, Yuan D, Guo C, Wang J (2020) Anisotropic mechanical properties and deformation behavior of low-carbon high-strength steel component fabricated by wire and arc additive manufacturing. *Mater Sci Eng A* 787:139514. <https://doi.org/10.1016/j.msea.2020.139514>
11. Le VT, Paris H (2021) On the use of gas-metal-arc-welding additive manufacturing for repurposing of low-carbon steel components: microstructures and mechanical properties. *Weld World* 65:157–166. <https://doi.org/10.1007/s40194-020-01005-y>
12. Le VT, Mai DS, Hoang QH (2020) A study on wire and arc additive manufacturing of low-carbon steel components: process stability, microstructural and mechanical properties. *J Braz Soc Mech Sci Eng* 42:480. <https://doi.org/10.1007/s40430-020-02567-0>
13. Aldalur E, Veiga F, Suárez A, Bilbao J, Lamikiz A (2020) Analysis of the wall geometry with different strategies for high deposition wire arc additive manufacturing of mild steel. *Metals* 10:892. <https://doi.org/10.3390/met10070892>
14. Plangger J, Schabhüttel P, Vuherer T, Enzinger N (2019) CMT additive manufacturing of a high strength steel alloy for application in crane construction. *Metals* 9:650. <https://doi.org/10.3390/met9060650>
15. Silwal B, Nycz A, Masuo CJ, Noakes MW, Marsh D, Vaughan D (2020) An experimental investigation of the effectiveness of Ar-CO₂ shielding gas mixture for the wire arc additive process. *Int J Adv Manuf Technol* 108:1285–1296. <https://doi.org/10.1007/s00170-020-05395-7>
16. Rafieezad M, Ghaffari M, Nemani AV, Nasiri A (2019) Microstructural evolution and mechanical properties of a low-carbon low-alloy steel produced by wire arc additive manufacturing. *Int J Adv Manuf Technol* 105:2121–2134. <https://doi.org/10.1007/s00170-019-04393-8>
17. İpekoğlu G, Küçükömeroğlu T, Aktarer SM, Sekban DM, Çam G (2019) Investigation of microstructure and mechanical properties of friction stir welded dissimilar St37/St52 joints. *Mater Res Express* 6(4):046537. <https://doi.org/10.1088/2053-1591/aafb9f>
18. Rodrigues TA, Duarte VR, Tomás D, Avila JA, Escobar JD, Rossinyol R, Schell N, Santos TG, Oliveira JP (2020) In-situ strengthening of a high strength low alloy steel during wire and arc additive manufacturing (WAAM). *Addit Manuf* 34:101200. <https://doi.org/10.1016/j.addma.2020.101200>
19. Moore P, Addison A, Nowak-Coventry M (2019) Mechanical properties of wire plus arc additive manufactured steel and stainless steel structures. *Weld World* 63:1521–1530. <https://doi.org/10.1007/s40194-019-00775-4>
20. Gürol U, Turgut B, Güleçyüz N, Dilibal S, Koçak M (2021) Development of multi-material components via robotic wire arc additive manufacturing. *Int J Print Technol Digit Ind* 5:721–729. <https://doi.org/10.46519/ij3dptdi.1033374>
21. Rodrigues TA, Duarte V, Avila JA, Santos TG, Miranda RM, Oliveira JP (2019) Wire and arc additive manufacturing of HSLA steel: effect of thermal cycles on microstructure and mechanical properties. *Addit Manuf* 27:440–450. <https://doi.org/10.1016/j.addma.2019.03.029>
22. Müller J, Hensel J, Dilger K (2022) Mechanical properties of wire and arc additively manufactured high strength steel structures. *Weld World* 66:395–407. <https://doi.org/10.1007/s40194-021-01204-1>
23. Fang Q, Zhao L, Liu B, Chen C, Peng Y, Tian Z, Yin F (2022) Microstructure and mechanical properties of 800-MPa-Class high-strength low-alloy steel part fabricated by wire arc additive manufacturing. *J Mater Eng Perform* 31:7461–7471. <https://doi.org/10.1007/s11665-022-06784-7>
24. Krauss G (1999) Martensite in steel: strength and structure. *Mater Sci Eng A* 273–275:40–57. [https://doi.org/10.1016/S0921-5093\(99\)00288-9](https://doi.org/10.1016/S0921-5093(99)00288-9)
25. EN 10025–2, Hot rolled products of structural steels - part 2: technical delivery conditions for non-alloy structural steels
26. EN 10025–6, Hot rolled products of structural steels - part 6: technical delivery conditions for flat products of high yield strength structural steels in the quenched and tempered condition

Publisher's note Springer Nature remains neutral with regard to jurisdictional claims in published maps and institutional affiliations.

Springer Nature or its licensor (e.g. a society or other partner) holds exclusive rights to this article under a publishing agreement with the author(s) or other rightsholder(s); author self-archiving of the accepted manuscript version of this article is solely governed by the terms of such publishing agreement and applicable law.